The Addition of Copper Nanoparticles to Mineral Trioxide Aggregate for Improving the Physical and Antibacterial Properties

Muhammad Akram Fakhriza[1], Bambang Rusdiarso[1], Siti Sunarintyas[2], and Nuryono Nuryono[1*]

[1]*Department of Chemistry, Faculty of Mathematics and Natural Sciences, Universitas Gadjah Mada, Sekip Utara, Yogyakarta 55281, Indonesia*

[2]*Department of Biomaterial, Faculty of Dentistry, Universitas Gadjah Mada, Jl. Denta 1, Sekip Utara, Yogyakarta 55281, Indonesia*

* ***Corresponding author:***

email: nuryono_mipa@ugm.ac.id

Received: November 28, 2022
Accepted: May 25, 2023

DOI: 10.22146/ijc.79491

Abstract: *The physical and antibacterial properties of mineral trioxide aggregate (MTA) have been improved by adding copper nanoparticles (CuNP). The CuNP colloid was synthesized by reacting $CuCl_2{\cdot}2H_2O$ and $NaBH_4$ as the reducing agent using $C_6H_8O_6$ as the capping agent. The Cu(II) concentration was varied by 3.0, 6.0, and 9.0 mM to produce CuNP-3, CuNP-6, and CuNP-9 colloids, respectively. The CuNP colloids were characterized with a UV-Vis spectrophotometer and TEM. MTA was hydrated with CuNP at a mass-to-volume ratio of 2:1 to produce Cu-MTA-3, Cu-MTA-6, and Cu-MTA-9, respectively. All products were characterized with XRD and SEM-EDX. The compressive strength, pH, Ca ion release, and solubility were measured, and antibacterial activity was tested. The results showed a spherical shape of the synthesized CuNP with a particle size of ~28.08 nm. Adding CuNP-9 to hydrated MTA increased the compressive strength, pH, Ca ion release, and solubility, with the value of 4.78±0.38 MPa; 9.01±0.03; 1718±63 ppm, and 22.48±0.37%, respectively. The highest antibacterial activity occurred for Cu-MTA-9, with an inhibition zone of 10.15±0.47 mm against* S. aureus *and 11.93±1.16 mm against* P. aeruginosa*. The findings show a potential application of the product for endodontic materials containing antibacterial agents.*

Keywords: *antibacterial; copper nanoparticles; physical properties; MTA*

■ INTRODUCTION

Inflammation in the dental root canal is one of the problems often found in dental and oral health [1], and mineral trioxide aggregate (MTA) is alternative endodontic material to solve the problem by treating the root canal of teeth [2]. MTA is divided into white mineral trioxide aggregate (WMTA) and gray mineral trioxide aggregate (GMTA). WMTA contains a small amount of iron oxide, so it does not cause discoloration of the teeth [3]. MTA meets the criteria as an endodontic material but has some low physical properties compared to other materials. MTA compressive strength is lower than biodentine in 1 to 28 d [4], and biodentine has a pH value of 12, while MTA has a lower pH [5].

Additionally, MTA does not show higher antibacterial properties against *S. aureus* bacteria, which are lower than other endodontic materials, namely AH-26 sealer [6]. Smart paste Bio and AH-Plus have higher antibacterial properties than MTA against *P. aeruginosa* [7]. Therefore, modifications of MTA are needed to improve the physical and antibacterial properties.

Copper nanoparticles (CuNP) have been widely reported to be able to act as antibacterial, for example, against *S. aureus* [8] and *P. aeruginosa* [9]. Nazer et al. [10] reported the addition of copper to Portland cement increases the pH of cement. Additionally, the Portland cement strength increased with copper addition because copper binds the material in the pores of the cement during the hydration process [11]. As MTA contains similar components to cement [12], the mechanical and antibacterial properties can be improved by modifying the metal and oxide nanoparticles. Yuliatun et al. [13]

reported the addition of SrO 5% and hydroxyapatite 6% increased the compressive strength of MTA from 2.21 to 18.01 MPa and improved the adhesion between dentin surface and MTA. Lim and Yoo [14] reported the modification of MTA with calcium fluoride (CaF_2) to give antibacterial activity against *Enterococcus faecalis*, *Porphyromonas endodontalis*, and *Porphyromonas gingivalis*. Bolhari et al. [15] improved the antibacterial activity of MTA by mixing MTA with fluorohydroxyapatite against *E. faecalis*. However, the effect of the modification on the mechanical properties was not investigated.

This paper reports the effect of CuNP addition on the hydrated MTA's physical properties and antibacterial activity. It included the synthesis of CuNP colloid and hydration of MTA using CuNP colloid as the hydrating liquid. The compressive strength and antibacterial activity against *S. aureus* and *P. aeruginosa* are also evaluated.

■ EXPERIMENTAL SECTION

Materials

Materials used for the synthesis of CuNP and Cu-MTA included copper(II) chloride dihydrate ($CuCl_2{\cdot}2H_2O$) p.a. (Pudak), L-ascorbic acid ($C_6H_8O_6$) p.a. (Merck), sodium borohydride ($NaBH_4$) p.a. (Merck). A sample of MTA was purchased from Maarc Dental. Chloramphenicol (Merck) was used as a positive control of the antibacterial agent, and bacteria of *P. aeruginosa* ATCC 27853 and *S. aureus* ATCC 29213 were provided by Laboratory of Microbiology, Universitas Gadjah Mada.

Instrumentation

CuNPs were characterized by a UV-Visible spectrophotometer (Genesys 10S). The morphology and the particle size of CuNP-6 were analyzed with Transmission Electron Microscope (TEM, JEOL JEM-1400). MTA before and after hydration, Cu-MTA-6 and Cu-MTA-9, were characterized with an X-ray Diffractometer (XRD, Shimadzu 6000, equipped with monochromatic Cu Kα radiation operated at 30 kW, $\lambda = 1.54$ Å) and scanned in the range of $3° \leq 2\theta \leq 90°$ with a scan speed of 3°/min (a scan step degree of 0.02°) and scanning electron microscope-energy dispersive X-ray (SEM EDX, JSM-6510LA). The compressive strength of the pellets was measured with a universal testing machine (UTM, Zwick BL-GR5500N) at the initial conditions: a force of 0.01 N, pre-load speed of 300 mm/min, and a test speed of 10 mm/min. The pH was measured with a pH meter (Inolab ph7110) while atomic absorption spectroscopy (AAS, ContrAA300 Analytik Jena) was used to determine the concentration of Ca(II) ions released from the MTA.

Procedure

Synthesis of copper nanoparticles

The precursor of $CuCl_2{\cdot}2H_2O$ (7.7, 15.4, and 23.0 mg) was dissolved in 7.5 mL of deionized water to produce Cu(II) solution with various concentrations (3, 6, and 9 mM). L-ascorbic acid (142.7 mg) was dissolved in 3.0 mL of deionized water, and then the solution was added to the Cu(II) solution and stirred with a magnetic stirrer for one hour at room temperature (25 °C). After that, $NaBH_4$ solids (3.4, 6.8, and 10.2 mg) were dissolved in 4.5 mL of deionized water and then added to the Cu(II) solutions with the various concentrations (3, 6, and 9 mM), and the solutions were stirred for 15 min at room temperature. The colloids of CuNP formed were successively labeled CuNP-3, CuNP-6, and CuNP-9. All CuNP colloids were characterized with a UV-Visible spectrophotometer. The morphology and particle size of CuNP-6 were analyzed with TEM.

Synthesis of Cu-MTA

MTA sample (1.00 g) was mixed with 0.50 mL of CuNP-3 colloid (the mass-to-volume ratio of 2:1). The mixture was stirred until it began to form a Cu-MTA-3 hard solid. Similar work was carried out for the CuNP-6 and CuNP-9 colloids to produce Cu-MTA-6 and Cu-MTA-9 solids, respectively, and hydration of MTA using deionized water was also performed. The products were characterized with XRD and SEM EDX.

Compressive strength testing

The four samples were (1) hydrated MTA; (2) Cu-MTA-3; (3) Cu-MTA-6; and (4) Cu-MTA-9 molded pellet tubes with sizes (diameter = 4 mm, thickness/height = 6 mm) on the mold as per ISO 9917-1. Pellets were stored in an airtight container at room temperature for 14 d. The compressive strength of the pellets was measured with a Universal Testing Machine.

Measurement of pH and Ca(II) ions release

The four samples of freshly hydrated MTA have formed pellets (diameter = 4 mm, height = 3 mm) and were then allowed to stand for 14 d at room temperature in an airtight container. The sample (60 mg) was immersed in 2.5 mL of demineralized water, which was replaced every 1, 3, and 7 d. The pH of the filtrate was measured with a pH meter, and Ca(II) ions concentrations were determined with AAS.

Solubility

The hydrated MTA sample used to identify the pH change and Ca(II) ions release was soaked for 7 d, separated from the filtrate, and dried in an oven at 50 °C for 6 h. The dried samples were weighed, and the difference in mass before and after immersion was calculated. The mass difference indicates the mass loss of the component from the sample [16]. The solubility of the sample was calculated using Eq. (1).

$$\text{Solubility} = \frac{\text{mass difference of the sample} - \text{evaporating hydrate mass}}{\text{sample mass before soaking}} \times 100\% \quad (1)$$

Antibacterial test

Four MTA samples were pelleted (diameter = 4 mm; thickness = 3 mm) and allowed to stand for 14 d in an airtight container. *S. aureus* bacteria were inoculated into sterile aqueducts and homogenized with a vortex, and 100 microliths were taken and put into the medium on a petri dish. The MTA sample was fed into the substrate in a saucer with tweezers. Disc paper was taken, and then a positive control (chloramphenicol) of 10 microliths was transferred to the disc paper. Disc paper was inserted into the substrate, and Petri dishes were covered with a seal and incubated for 24 h. The same work was performed for samples of Cu-MTA-3, Cu-MTA-6, and Cu-MTA-9, as well as *P. aeruginosa* bacteria. Observations and measurements of antibacterial activity were carried out the next day. Antibacterial activity was calculated by measuring the diameter of the inhibitory power of bacteria in a saucer with calipers or rulers. The test was conducted at the Microbiology Laboratory, Faculty of Biology, Universitas Gadjah Mada.

■ RESULTS AND DISCUSSION

Characteristics of CuNP

The precursor used to prepare CuNP colloids was a blue color Cu(II) solution obtained by dissolving $CuCl_2{\cdot}6H_2O$. Adding an L-ascorbic acid and $NaBH_4$ solution to the Cu(II) solution changes the solution to yellow-brown, as seen in Fig. 1.

The results of synthesized CuNP were brownish-yellow colloids, similar to the results reported previously [17]. The intensity increases as the concentration of CuNP increases (from left to right), indicating a higher concentration of CuNP. The absorbance of the CuNP colloids is presented in Fig. 2. All the maximum wavelengths in a 300–305 nm range align with previous research [18]. An increase of Cu(II) concentrations from 3.0 to 6.0 mM increases the absorbance significantly, and the increase from 6.0 to 9.0 mM slightly increases the absorbance. Therefore, 6.0 mM was chosen as the representation for TEM characterization.

Characterization was continued to identify the morphology of CuNP with TEM, and CuNP-6 is the representative sample to know the particle size. The result can be seen in Fig. 3. The TEM image showed that the main morphology of CuNP-6 tends to be spherical, and based on Fig. 3(a), particle size can be measured by taking and analyzing 45 points in the TEM image using

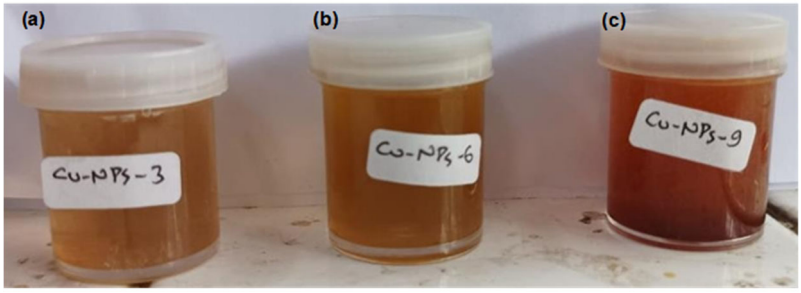

Fig 1. CuNP images synthesized from Cu(II) solution with a concentration of (a) 3.0 mM, (b) 6.0 mM, and (c) 9.0 mM

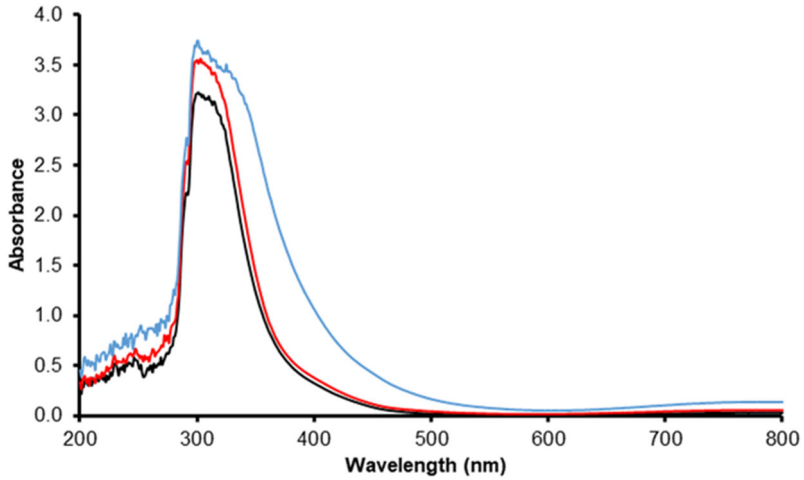

Fig 2. UV-Visible Spectra of CuNP colloids

ImageJ and OriginPro software. The histogram of the CuNP-6 particle size distribution is presented in Fig. 3(b), with an average of 28.08 nm.

Characteristics of MTA-CuNP

For hydration, 1 g of MTA powder was mixed with 0.5 mL of CuNP colloid (the mass-to-volume ratio of 2:1). It follows the hydration procedure for any commercial MTA. Characterization with the XRD instrument was performed on MTA, hydrated MTA, Cu-MTA-6, and Cu-MTA-9, and the patterns are presented in Fig. 4. Referring Crystallography Open Database (COD) and the value of 2θ, five components, namely C_2S, C_3S, C_3A, CaO, and Ta_2O_3 for MTA, and the presence of CuNPs for Cu-MTA can be obtained and presented in Table 1. Products of the hydration include calcium silicate hydrate (C-S-H),

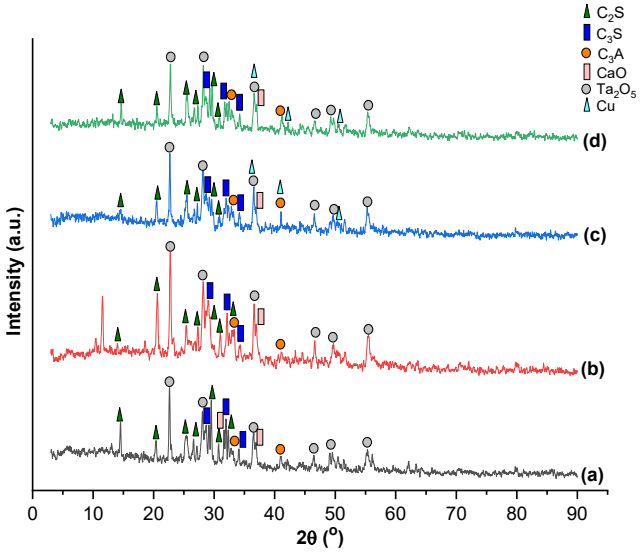

Fig 4. XRD pattern of (a) MTA, (b) Hydrated MTA, (c) Cu-MTA-6, and (d) Cu-MTA-9

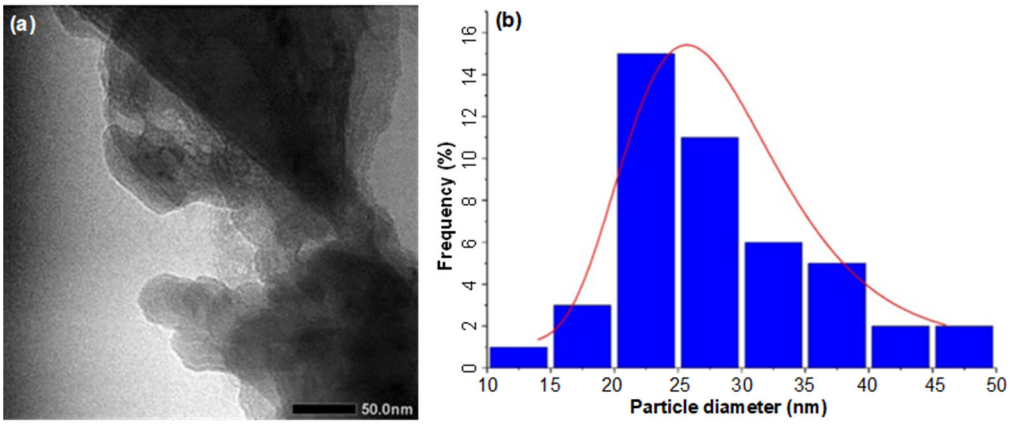

Fig 3. (a) TEM image and (b) particle size distribution histogram of CuNP-6

Table 1. Value 2θ peaks of XRD patterns

Composition	2θ (°)			
	Non-hydrated MTA	Hydrated MTA	Cu-MTA-6	Cu-MTA-9
C_2S (COD	14.54	14.06	14.52	14.64
00-210-3316)	20.40	20.64	20.48	20.56
	27.18	27.32	27.24	27.30
	29.54	29.32	29.56	29.68
	30.78	31.04	30.92	30.96
C_3S (COD	29.20	29.06	29.16	29.24
00-154-0704)	32.00	32.14	32.04	32.10
	34.12	34.30	34.24	34.28
C_3A (COD	33.12	33.30	32.92	32.98
00-901-4359)	40.96	40.62	41.04	41.14
CaO (COD	36.84	37.00	36.94	37.04
00-900-6701)				
Ta_2O_5 (COD	22.66	22.76	22.70	22.80
00-153-1068)	28.06	28.16	28.16	28.20
	36.58	36.60	36.56	36.62
	46.52	46.62	46.54	46.56
	49.58	49.70	49.68	49.74
	55.32	55.50	55.28	55.36
Cu (JCPDS			36.64	37.00
01-089-2838)			41.10	41.30
			50.62	50.64

calcium hydroxide (CH), monosulfate phase, and ettringite ($3CaO{\cdot}Al_2O_3{\cdot}3CaSO_4{\cdot}31H_2O$), supporting the previous report [19]. The peaks of CuNP are too low and are covered by the peaks of other components because the CuNP used is so tiny that the intensity is small and difficult to identify.

The intensity of C2S and C3S peaks in hydrated MTA, Cu-MTA-6, and Cu-MTA-9 is lower than in non-hydrated MTA. It is probable the water forms hydrated C_2S and C_3S that reduce the crystallinity [20]. Adding CuNP to the MTA (in Cu-MTA-6 and Cu-MTA-9 samples) reduces the intensity of C_2S and C_3S because the nanoparticles can provide more nucleation additional sites for the crystallization of calcium silicate hydrate and calcium hydroxide, which are hydration products replacing C_2S and C_3S [21].

Characterization was followed by an analysis of MTA, hydrated MTA, Cu-MTA-3, Cu-MTA-6, and Cu-MTA-9 samples using SEM-EDX instruments, as shown in Fig. 5. SEM images of MTA (Fig. 5(a)) still show a large enough space when compared to MTA hydrated (Fig. 5(b)) because C-S-H formed during hydration strengthens and makes the strong interaction between particles [22]. The addition of CuNP makes the sample density increase since a small-sized CuNP (~28.08 nm) can fill the empty pores of the MTA, as seen in Cu-MTA-3 (Fig. 5(c)), Cu-MTA-6 (Fig. 5(d)), and Cu-MTA-9 (Fig. 5(e)). The sample density increases as the concentration of CuNP increases, indicating more CuNP can fill the space in the pores of the MTA sample. Testing continued using EDX, which showed the percentage of the composition of the elements in the sample in Table 2. The presence of CuNP, which is difficult to be confirmed with XRD, can be overcome with EDX data. CuNP of 1.87 to 2.95% of the mass can be found in Cu-MTA samples.

Compressive strength testing is one of the basic tests to be carried out because compressive strength indicates the MTA setting reaction and stability [23]. The results of compressive strength tests on the MTA,

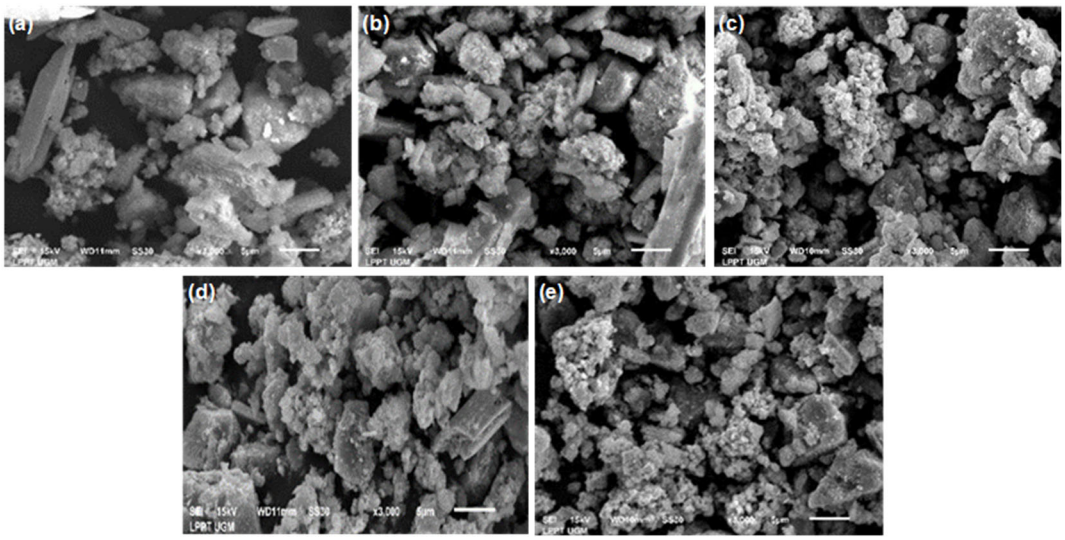

Fig 5. SEM image of 3000× magnification at (a) MTA, (b) MTA hydrated, (c) Cu-MTA-3, (d) Cu-MTA-6, and (e) Cu-MTA-9

Table 2. Mass percentage composition of all samples

Element	Mass (%)				
	MTA	MTA hydrated	Cu-MTA-3	Cu-MTA-6	Cu-MTA-9
O	34.54	34.00	38.99	45.21	39.19
Al	0.36	0.32	0.79	0.88	0.87
Si	1.25	0.79	3.40	3.33	3.33
Ca	27.41	9.77	21.24	25.12	21.35
Ta	36.44	55.00	33.71	22.67	31.81
Cu	-	-	1.87	2.79	2.95

Table 3. Compressive strength of samples after hydration for 14 days

Sample name	Compressive strength (MPa)
MTA	3.87±0.13
Cu-MTA-3	4.04±0.65
Cu-MTA-6	4.42±0.22
Cu-MTA-9	4.74±0.38

Cu-MTA-3, Cu-MTA-6, and Cu-MTA-9 are found in Table 3.

Table 3 shows that adding CuNP to the MTA increases the material's compressive strength, per previous research [24]. Adding copper to Portland cement can improve the cement's strength because the pores in the cement are filled with copper, which functions as a binder to the material during the hydration process [10]. The addition of nanoparticles to cement strengthens the structure of the cement because the nanoparticles act as pore fillers, so there is a significant increase in cement density [25]. The rise in CuNP concentration causes the compressive strength value to be higher because more CuNP fills the pores in the MTA so that the density of the MTA increases. The results of the SEM-EDX analysis in Fig. 5 support the compressive strength because they show a greater morphological density of the sample as the increase of added CuNP concentrations.

The pH change was evaluated to determine the MTA's and Cu-MTA's alkalinity, which affects antibacterial properties [26]. The pH change in various hydration periods is presented in Table 4.

The highest pH is generated when the soaking of the sample is carried out on the first day, then decreases further and stabilizes at the alkaline pH from day 3 to 7. The obtained results follow the previous research [27-28]. The decrease in pH is relatively low to lead to a stable pH

Table 4. Result of pH test on MTA and Cu-MTA samples

Sample name	Days		
	1	3	7
MTA	8.55±0.05	7.96±0.16	7.83±0.01
Cu-MTA-3	9.01±0.03	8.19±0.03	8.13±0.01
Cu-MTA-6	8.73±0.09	8.07±0.07	8.03±0.07
Cu-MTA-9	8.68±0.09	8.02±0.10	7.94±0.05

the overtime the MTA material, and the variation of Cu-MTA will experience an increase in mechanical properties, causing the release of hydroxide ions into the environment to be reduced until it begins to stabilize [28]. The pH value obtained is already alkaline, so it is expected to be able to contribute to antibacterial properties.

The diffusion of Ca(II) ions from MTA, Cu-MTA-3, Cu-MTA-6, and Cu-MTA-9 was evaluated because calcium is the main component in MTA, namely C_2S, C_3S, C_3A, and CaO [22]. The test results are shown in Fig. 6. It can be seen that the highest release of Ca(II) ions for all samples occurs on the first day of immersion and then decreases on the next day, and it follows previous research [28]. The diffusion of Ca(II) ions correlates with the pH value because in forming hydration products in the form of C-S-H, $Ca(OH)_2$ compounds are also produced, which will be ionized and are responsible for the diffusion of Ca(II) ions, and the resulting pH value. An increase in the concentration of Ca(II) ions leads to a higher resulting pH value [27]. This can be proved by comparing Table 4 and Fig. 6, which have similarities in the sample order. Material Cu-MTA-3 has the highest diffusion of Ca(II) ions because using CuNP accelerates the hydration process, resulting in more hydration products, especially $Ca(OH)_2$ [21], so there is an increase in Ca cations from the MTA material. This reason also can be applied to Cu-MTA-6 and Cu-MTA-9. Both variations have more CuNP concentrations that can cover the pores where Ca(II) ions come out. This statement can be proven by the SEM-EDX image (Fig. 5), which shows that the presence of CuNP in MTA increases the density (small pores). The lost calcium is used to prevent dental demineralization, accelerate tooth mineralization, and repair and regenerate bone damage [29].

Solubility testing aims to evaluate the stability of MTA and Cu-MTA samples in an aqueous solution. The solubility of MTA, Cu-MTA-3, Cu-MTA-6, and Cu-MTA-9 samples are presented in Table 5.

The solubility of Cu-MTA samples is higher than MTA because CuNP can accelerate the hydration resulting in more $Ca(OH)_2$ as a hydration product. One of the ionization results of $Ca(OH)_2$ is the Ca(II) cation which is the main constituent component of the MTA, so when the Ca(II) is released from the MTA, it increases in the solubility of the Cu-MTA. The study results follow the results obtained from pH testing and diffusion of Ca(II) ions. High solubility values not only have a negative

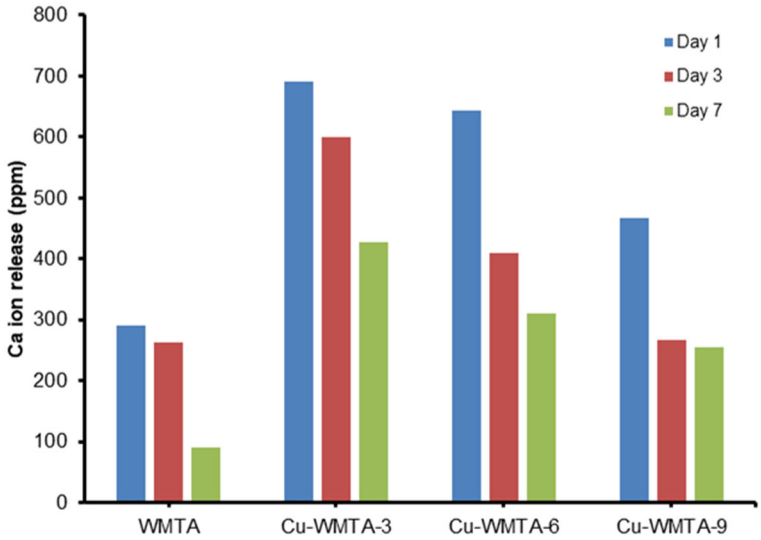

Fig 6. Diagram of Ca(II) ion released from MTA samples after various days of hydration

Table 5. The solubility of MTA samples after 14 days of hydration

Sample name	Solubility	
	Mass (mg)*	Percentage (%)**
MTA	10.19±0.53	17.00±0.96
Cu-MTA-3	14.05±0.57	22.48±0.37
Cu-MTA-6	12.06±0.28	20.68±0.61
Cu-MTA-9	11.29±0.24	19.08±0.54

*the mass of the initial sample minus the mass of the final sample (after soaking)

**Percentage of the dissolved mass to the mass of the initial sample

impact on the teeth but also have some positive benefits. $Ca(OH)_2$ can reduce inflammatory processes, dissolve dead dental tissue, and heal periapical tissue in the teeth [30].

The antibacterial properties test aims to evaluate the effect of adding CuNP with various concentrations on the MTA antibacterial activity. The bacteria investigated are *S. aureus*, a Gram-positive bacteria, and *P. aeruginosa*, a Gram-negative bacteria. Both are found in teeth [31]. The results of testing the antibacterial properties, presented as inhibition zones, of MTA, Cu-MTA-3, Cu-MTA-6, and Cu-MTA-9 can be seen in Fig. 7 for *S. aureus* bacteria and Fig. 8 for *P. aeruginosa* bacteria. Observations were made on MTA samples on the 7th day after hydration.

The inhibition zone diameters of the antibacterial test presented in Fig. 7 and 8 were measured using calipers, and the result is summarized in Table 6.

Table 6 shows that MTA does not have inhibitory capability against both *S. aureus* and *P. aeruginosa* bacteria. There is no component in MTA acting as the antibacterial agent, and the pH of MTA is around 8 and 9 (Table 4). Both bacteria, *S. aureus,* and *P. aeruginosa*, still grow in the pH range of 4.0 to 9.8 [32-33]. CuNP, an antibacterial agent [34], is still active even though combined with MTA. The antibacterial performance mechanism is probably different from MTA modified with CaF_2 [14] and fluorohydroxiapatite [15], in which the higher pH leads to bacterial death. The CuNP on the MTA surface may interact with the bacterial cells causing bacterial cell leakage and leading to lysed and death [35].

Table 6. The results of the measurement of the inhibition zone of the MTA and Cu-MTA samples

Sample name	Inhibition zone (mm)	
	S. aureus	*P. aeruginosa*
MTA	0	0
Chloramphenicol	25.17±1.31	27.00±1.41
Cu-MTA-3	8.30±0.53	8.42±0.78
Cu-MTA-6	9.20±0.25	9.74±0.88
Cu-MTA-9	10.15±0.47	11.93±1.16

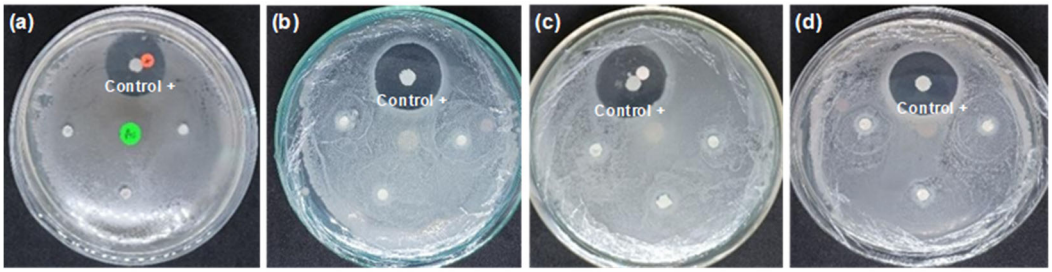

Fig 7. Inhibition zone of *S. aureus* tested with (a) MTA; (b) Cu-MTA-3; (c) Cu-MTA-6; (d) Cu-MTA-9

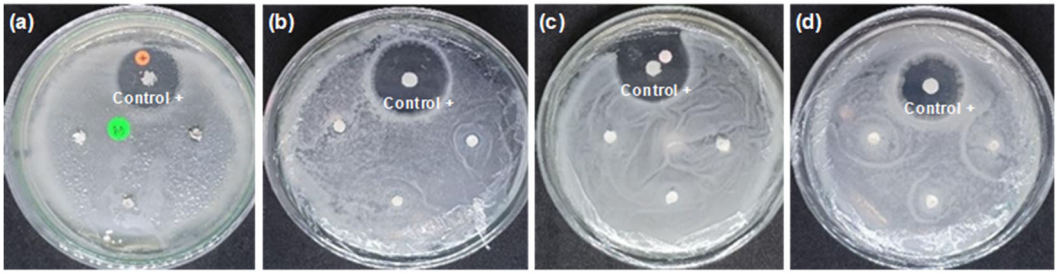

Fig 8. Inhibition zone of *P. aeruginosa* tested with (a) MTA; (b) Cu-MTA-3; (c) Cu-MTA-6; (d) Cu-MTA-9

Yadav et al. [34] reported that CuNP interacts with DNA and the protoplasm of bacterial cells, causing DNA damage, and bacteria cannot carry out cell metabolism.

■ CONCLUSION

Copper nanoparticles have been successfully synthesized by reacting the precursors of $CuCl_2{\cdot}2H_2O$, the protective agent of L-ascorbic acid, and $NaBH_4$, as a reducing agent, to produce spherical CuNP with the particle size of ~28.08 nm. Hydration of MTA with CuNP colloid improved the compressive strength, pH, Ca(II) ions release, solubility, and antibacterial properties. Using CuNP colloid prepared from 9.0 mM Cu(II) solution increased the compressive strength from 4 to 4.74 MPa and showed antibacterial activity with the inhibitor zone diameters of 10.15 mm for *S. aureus* bacteria and 11.93 mm for *P. aeruginosa*. The modified MTA is the potential to be implemented for endodontic material containing antibacterial agents.

■ ACKNOWLEDGMENTS

The authors would like to thank the Research Directorate, Universitas Gadjah Mada, through the research grant *Penelitian Dasar Unggulan Perguruan Tinggi* (PDUPT), contract number: 1651/UN1/DITLIT/Dit-Lit/PT.01.03/2022 for the financial support.

■ REFERENCES

[1] Napitupulu, R.L.Y., Adhani, R., and Erlita, I., 2019, Hubungan perilaku menyikat gigi, keasaman air, pelayanan kesehatan gigi terhadap karies di MAN 2 Batola, *Dentin*, 1 (3), 17–22.

[2] Bachtiar, Z.A., 2016, Perawatan saluran akar pada gigi permanen anak dengan bahan gutta percha, *Jurnal PDGI*, 2 (65), 60–67.

[3] Patel, N., Patel, K., Baba, S.M., Jaiswal, S., Venkataraghavan, K., and Jani, M., 2014, Comparing gray and white mineral trioxide aggregate as a repair material for furcation perforation: An *in vitro* dye extraction study, *J. Clin. Diagn. Res.*, 8 (10), ZC70–ZC73.

[4] Butt, N., Talwar, S., Chaudhry, S., Nawal, R.R., Yadav, S., and Bali, A., 2017, Comparison of physical and mechanical properties of mineral trioxide aggregate and biodentine, *Indian J. Dent. Res.*, 25 (6), 692–697.

[5] Kaur, M., Singh, H., Dhillon, J.S., Batra, M., and Saini, M., 2017, MTA versus biodentine: Review of literature with a comparative analysis, *J. Clin. Diagn. Res.*, 11 (8), ZG01–ZG05.

[6] Mohammadi, Z., Giardino, L., Palazzi, F., and Shalavi, S., 2012, Antibacterial activity of a new mineral trioxide aggregate-based root canal sealer, *Int. Dent. J.*, 62 (2), 70–73.

[7] Gürel, M., Demiryürek, E.Ö., Özyürek, T., and Gülhan, T., 2016, Antimicrobial activities of different bioceramic root canal sealers on various bacterial species, *Int. J. Appl. Dent. Sci.*, 2, 19–22.

[8] Akhidime, D., Saubade, F., Benson, P., Butler, J., Olivier, S., Kelly, P., Verran, J., and Whitehead, K., 2018, The antimicrobial effect of metal substrates on food pathogens, *Food Bioprod. Process.*, 113, 68–76.

[9] Ghasemian, E., Naghoni, A., Rahvar, H., Kialha, M., and Tabaraie, B., 2015, Evaluating the effect of copper nanoparticles in inhibiting *Pseudomonas aeruginosa* and *Listeria monogtogenes* biofilm formation, *Jundishapur J. Microbiol.*, 8 (5), e17430.

[10] Nazer, A., Payá, J., Borrachero, M.V., and Monzó, J., 2016, Use of ancient copper slags in Portland cement and alkali activated cement matrices, *J. Environ. Manage.*, 167, 115–123.

[11] Liu, S., Li, Q., and Zhao, X., 2018, Hydration kinetics of composite cementitious materials containing copper tailing powder and graphene oxide, *Materials,* 11 (12), 2499.

[12] Saghiri, M.A., Kazerani, H., Morgano, S.M., and Gutmann, J.L., 2020, Evaluation of mechanical activation and chemical synthesis for particle size modification of white mineral trioxide aggregate, *Eur. Endod. J.*, 5 (2), 128–133.

[13] Yuliatun, L., Kunarti, E.S., Widjijono, W., and Nuryono, N., 2022, Enhancing compressive strength and dentin interaction of mineral trioxide aggregate by adding SrO and hydroxyapatite, *Indones. J. Chem.*, 22 (6), 1651–1662.

[14] Lim, M., and Yoo, S., 2022, The antibacterial activity of mineral trioxide aggregate containing calcium fluoride, *J. Dent. Sci.*, 17 (2), 836–841.

[15] Bolhari, B., Sooratgar, A. Pourhajibagher, M., Chitsaz, N., and Hamraz, I., 2021, Evaluation of the antimicrobial effect of mineral trioxide aggregate mixed with fluorohydroxyapatite against *E. faecalis in vitro*, *Sci. World J.*, 2021, 6318690.

[16] Pushpa, S., Maheshwari, C., Maheshwari, G., Sridevi, N., Duggal, P., and Ahuja, P., 2018, Effect of pH on solubility of white mineral trioxide aggregate and biodentine: An *in vitro* study, *J. Dent. Res. Dent. Clin. Dent. Prospects*, 12 (3), 201–207.

[17] Cerda, J.S., Gomez, H.E., Nunez, G.A., Rivero, I.A., Ponce, Y.G., and Lopez, L.Z.F., 2017, A green synthesis of copper nanoparticles using native cyclodextrins as stabilizing agents, *J. Saudi Chem. Soc.*, 21 (3), 341–348.

[18] Suprapto, S., Handoyo, C.A.H., Senja, P.A., Ramadhan, VB, and Ni'mah, Y.L., 2020, synthesis of copper nanoparticles using *Chromolaena odorata* (L.) leaf extract as a stabilizing agent, *Indones. J. Chem. Anal.*, 3 (1), 9–16.

[19] Camilleri, J., 2007, Hydration mechanism of mineral trioxide aggregate, *Int. Endod. J.*, 40 (6), 462–470.

[20] Akhavan, H., Mohebbi, P., Firouzi, A., and Noroozi, M., 2015, X-ray Diffraction analysis of ProRoot mineral trioxide aggregate hydrated at different pH values, *Iran. Endod. J.*, 11 (2), 111–113.

[21] Wang, X., 2017, Effects of Nanoparticles on the Properties of Cement-Based Materials, *Dissertation*, Civil Engineering Iowa State University, Iowa, US.

[22] Altan, H., and Tosun, G., 2016, The setting mechanism of mineral trioxide aggregate, *J. Istanbul Univ. Fac. Dent.*, 50 (1), 65–72.

[23] Sobhnamayan, F., Adl, A., Shojaee, N.S., Sedigh-Shams, M., and Zarghami, E., 2017, Compressive strength of mineral trioxide aggregate and calcium-enriched mixture cement mixed with propylene glycol, *Iran. Endod. J.*, 12 (4), 493–496.

[24] Akbari, M., Zebarjad, S.M., Nategh, B., and Roubani, R., 2013, Effect of nano-silica on setting time and physical properties of mineral trioxide aggregate, *J. Endod.*, 39 (11), 1448–1451.

[25] Nazari, A., and Riahi, S., 2011, Effects of CuO nanoparticles on compressive strength of self-compacting concrete, *Sādhanā*, 36 (3), 371–391.

[26] Farrugia, C., Baca, P., Camilleri, J., and Arias Moliz, M.T., 2017, Antimicrobial activity of ProRoot MTA in contact with blood, *Sci. Rep.*, 7, 41359.

[27] Abu Zeid, S.T.H., Alothmani, O.S., and Yousef, M.K., 2015, Biodentine and mineral trioxide aggregate: An analysis of solubility, pH changes, and leaching element, *Life Sci. J.*, 12 (4), 18–23.

[28] Wibowo, M.W.A., Yunita, A.I., Mukaromah, L., Kartini, I., and Nuryono, N., 2022, Effect of titania and silver nanoparticles on the tensile strength of cement-like mineral trioxide aggregate, *Mater. Sci. Forum*, 1068, 183–188.

[29] Al-Sanabani, J.S., Madfa, A.A., and Al-Sanabani, F.A., 2013, Application of calcium phospate materials in dentistry, *Int. J. Biomater.*, 2013, 876132.

[30] Dewiyani, S., 2011, Calcium hydroxide as intracanal dressing for teeth with apical periodontitis, *Dent. J.*, 44 (1), 12–16.

[31] Yamin, I.F., and Natsir, N., 2014, Bakteri dominan di saluran akar gigi nekrosis, *Dentofasial*, 13 (2), 113–116.

[32] Valero, A., Pérez-Rodríguez, F., Carrasco, E., Fuentes-Alventosa, J.M., García-Gimeno, R.M., and Zurera, G., 2009, Modelling the growth boundaries of *Staphylococcus aureus*: Effect of temperature, pH and water activity, *Int. J. Food Microbiol.*, 133 (1-2), 186–194.

[33] Klein, S., Lorenzo, C., Hoffmann, S., Walther, J.M., Storbeck, S., Piekarski, T., Tindall, B.J., Wray, V., Nimtz, M., and Moser, J., 2009, Adaptation of *Pseudomonas aeruginosa* to various conditions includes tRNA-dependent formation of alanyl-phosphatidylglycerol, *Mol. Microbiol.*, 71 (3), 551–565.

[34] Yadav, L., Tripathi, R.M., Prasad, R., Pudake, R.N., and Mittal, J., 2017, Antibacterial Activity of Cu Nanoparticles against *E. coli*, *Staphylococcus aureus* and *Pseudomonas aeruginosa*, *Nano Biomed. Eng.*, 9 (1), 9–14.

[35] Brooks, G.F., Carroll, K.C., Butel, JS, and Morse, S.A., 2007, *Medical Microbiology*, McGraw-Hill Medical, New York, US.